JOURNAL OF MATERIALS SCIENCE 30 (1995) 1266–1272

Mechanical fatigue of epoxy resin

M. NAGASAWA,* H. KINUHATA, H. KOIZUKA, K. MIYAMOTO, T. TANAKA, H. KISHIMOTO
Toyota Technological Institute, Hisakata, Tempaku-ku, Nagoya, 468, Japan
T. KOIKE
Research and Development Laboratories, Yuka Shell Epoxy Co. Ltd. Shiohama-cho, Yokkaichi-shi, Mie, 510, Japan

In static bending fatigue tests, epoxy resins show practically no fatigue if the stress given to specimen is lower than a critical value, which is close to the bending strength of the specimen. In cyclic bending fatigue tests, on the other hand, the resins are easily fractured even though the stresses are far below the critical values. Some strain may be accumulated on the surface of specimen through cyclic deformations. However, the strain accumulated is reversible. If the specimen is allowed to rest, the strain disappears. If the strain reaches a critical value, an irreversible transition may be induced, probably in the arrangement of segments on the surface. A crack nucleus thus created may propagate and cause the final fracture of the specimen, following the fracture mechanics of elastic materials. The lifetime of epoxy resins under cyclic bending load is determined by the time required for creating a crack nucleus on surface.

1. Introduction

Despite the extensive investigations which are being carried out on the fatigue phenomena of epoxy resin composites with various kinds of fibres and other ingredients, the fatigue of epoxy resins themselves does not appear to have been fully studied. At least in cyclic fatigue tests of epoxy resins, fatigue phenomena appear to proceed in three different stages: nucleation of a crack, its propagation (slow crack growth) and final failure of the specimen, just as in other brittle materials [1]. The crack growth rate, da/dN, of epoxy resins has been well studied and was found to be correlated with stress intensity factor range, ΔK, by

$$\frac{da}{dN} = A\,\Delta K^n \tag{1}$$

where $\Delta K = K_{max} - K_{min}$, K_{max} and K_{min} being the maximum and minimum stress intensity factors, and A and n are constants, as in metals and other elastic materials. It is reported that the values of n for epoxy resins are much higher than the values commonly found for metals and other plastics [2–8], being as high as 10. [1–3] However, it appears to the present authors that the total behaviour of epoxy resins in fatigue behaviour has not fully been clarified. In particular, one of the most important unsolved problems in the fatigue phenomena of epoxy resins may be how fatigue crack initiation occurs after a period of repeated loading.

There are two different forms of mechanical fatigue, static fatigue which denotes the failure during a long period of constant loading, and cyclic fatigue which denotes the failure after a period of repeated loading. It is empirically known that epoxy resins are much more easily fractured under rotary-bending loading than under static loading. The difference is often explained by assuming that the surfaces of epoxy resins might have some fatal defects even if they are carefully polished. Then, the probability that a stress is focused on a fatal defect would be much higher in rotary-bending fatigue tests than in static bending fatigue tests. This speculation may be examined if we compare static bending fatigue tests with cyclic plane-bending fatigue tests for the same samples.

Moreover, in fatigue, many metals exhibit mechanical fatigue even if they have no fatal defects on their surfaces. Cracks are created on their surfaces due to repeated loadings, and it is now well established that the fatigue crack initiation is due to near-surface dislocation slip occurring in metal crystals [4]. No such dislocation slip, however, should occur in epoxy resins which are not only non-crystalline but also have three-dimensional network structures.

Here, it should be noted that we are interested in the mechanical fatigue of epoxy resins, which have three-dimensional network structures. In the case of thermoplastics made of uncross-linked polymer molecules, their mechanical properties are highly sensitive to temperature rise due to energy dissipation during cyclic loading, and creep may be involved in the fatigue process, considering that the fatigue of thermoplastic polymer materials is highly molecular weight dependent over a very wide range of molecular weight [5].

*Author to whom all correspondence should be addressed.

0022–2461

2. Experimental procedure

2.1. Samples

The epoxy resin samples used were provided from Yuka Shell Epoxy Co. Ltd. They were prepared by polymerization of mixtures of diglycidyl ether oligomers of *bis*-phenol-A (Epikote E825, E828 and E834) [6] and 3 or 4-methyl-1,2,3,6-tetrahydrophthalic anhydride (Epicure DX126) with addition of an accelerator, 2-ethyl-4-methylimidazole (Epicure EMI24) at 150 °C for 4 h in cylindrical test tubes of 15 mm diameter. The mixtures were evacuated at 100 °C for 2 h to remove dissolved air before polymerization. The mixing ratio of the reagents, as well as weight-average molecular weights, M_w, and molecular weight distribution indices, M_w/M_n, of the three oligomers (Epikotes) used are listed in Table I. Three oligomer samples of *bis*-phenol-A consist of almost the same chemical compositions and are different only in the repeating part. Their M_w and M_w/M_n were determined by gel permeation chromatography, using Model 600 of Waters Associates with a column system of G2500 and G3000H of Toso Co. Ltd, and standard polystyrenes as reference [6]. Difference in M_w of oligomers causes a difference in the degree of cross-linking and, consequently, in the number of main chains crossing unit cross-section in the samples. Most experiments in this work were carried out with sample E828. However, it was found that there were considerably large differences in their mechanical properties such as tensile strength between the samples of E828 prepared recently and several years ago. Quantitative comparisons were, therefore, limited within the data obtained with the same series of samples. The samples E828 prepared several years ago is denoted by E828-o.

Specimens with desired shapes for fatigue experiments were prepared by machining the epoxy resin rods with a lathe. The shapes and sizes of the specimens used for various measurements are shown in Fig. 1. The length of the centre part, l, in the upper figure was different for different purposes. The surface of each specimen was finished as smoothly as possible with sand papers of JIS 1000 and 1500 by moving the papers along the rod axis of the specimens, unless otherwise stated.

Some specimens of E828 were annealed in an oven in an argon atmosphere to change the packing state of segments. They were heated from 100 °C to 150 °C at a rate of 10 °C h^{-1} and kept at 150 °C for 3 h. Half of the specimens were removed from the oven and cooled in air as usual (sample E828-H2), while the other half were gradually cooled from 140 °C to 120 °C in the oven at a rate of 2 °C per day and then to 100 °C at a rate of 1 °C per day (sample E828-H1). The conditions for annealing were determined by taking into account the relaxation times of linear polymers in volume contraction [7]. The specimens were machined before annealing, but the surface finishing with no. 1500 sand papers was done after annealing. A quantitative change in the state of segment packing could not be detected by experiments in this work, but a clear difference was observed on the fracture surfaces of annealed and unannealed samples.

TABLE I Compositions of epoxy resins and molecular weights and oligomers

Reagents	E825	E828	E834
bis-phenol-A	100	100	100
Methyl tetrahydrophthalic anhydride	87	80	60
Accelerator	1	1	1
M_w of oligomer	354	388	590
M_w/M_n of oligomer	1.00	1.06	1.23

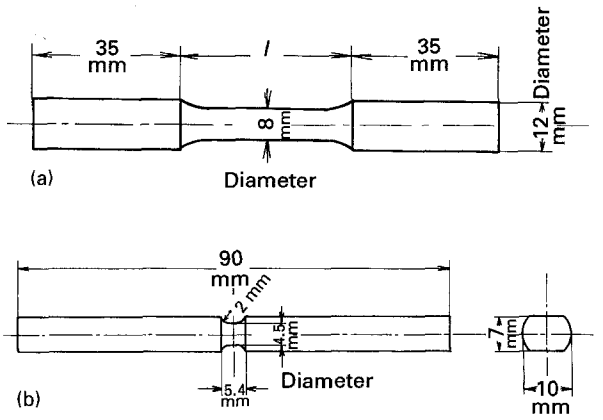

Figure 1 Test pieces for fatigue tests: (a) length, l, 40 mm for static and rotary bending tests and 18.5 mm for annealed specimens; (b) for cyclic plane-bending fatigue tests (stress concentration factor $\alpha = 1.28$).

2.2. Measurements

2.2.1. Cyclic fatigue

Rotary bending fatigue tests were carried out using a testing machine of Shimadzu Instruments, Ltd. In the instrument, specimens were loaded with uniform bending moments. The stress, σ, in the specimen may be calculated from the weight, P, and the dimensions of the specimen such as

$$\sigma = \frac{(1/2)P\ L}{(1/32)\ \pi\ d^3} \quad (2)$$

where d is the diameter at the centre, and L is the length of a moment arm in calculating the bending moment.

Specimens were installed with the help of a thin Teflon sheet to avoid fretting corrosion in collets. Deviation in the centre of the rotating rods was adjusted to be within 0.05 mm. The rotating specimen was covered with a polyvinyl chloride-coated cloth, so that the rotary tests could be carried out in an argon atmosphere and also at high temperatures. In experiments at high temperatures, specimens were fully preheated with steel clamps in a vacuum oven, and, after being installed in the test instrument, the surface of the specimen was kept at the desired temperature by blowing with air of the same temperature. The temperature on the surface of the specimen was monitored by an i.r. radiation thermometer. In most experiments, the rotation speeds were chosen to be 300 and 600 r.p.m. which were low enough not to cause serious temperature rise.

Cyclic plane-bending fatigue tests were carried out at 1800 cycles/min with a Shimadzu Instruments Ltd UF-15, with four-point bending loads.

2.2.2. Static fatigue

The time-to-failure, (t_f), through static loading was measured using part of a rotary-bending fatigue test instrument at almost the same experimental conditions as in rotary-bending fatigue tests.

2.2.3. Material characteristics of the samples

Tensile and bending strengths and also stress–strain relationships were determined with a Shimadzu Universal Testing Machine at room temperature. The crosshead speed was between 0.1 and 10 mm min^{-1} in tensile experiments and between 5 and 100 mm min^{-1} in bending experiments.

Unless otherwise stated, all tests in the present work were carried out in air at room temperature.

2.2.4. Observation of the fracture surface

Fracture surfaces were observed by a metallurgical microscope and a profile projector and also by a scanning electron microscopy (Hitachi S570). Thin films of gold were evaporated *in vacuo* on to fracture surfaces for electron microscopy. The magnification was usually 60–600. The depth and other dimensions of the slow crack growth area (sometimes called the mirror area) was determined from photographs or on the viewing screen of the profile projector.

3. Results

3.1. Material characteristics of the samples

Tensile and bending strengths of the samples somewhat depend on strain rate. They increase with increasing strain rates. The values obtained at a crosshead speed $\dot{\delta} = 1$ mm min^{-1} in tensile strength and at $\dot{\delta} = 5$ mm min^{-1} in bending strength are listed in Table II, for comparison. Meaningful differences in both tensile and bending strengths can be found among the samples having different degrees of cross-linking and also between the annealed and unannealed samples (sample E828-H1 and -H2).

The glass transition temperatures, T_g, of samples E828-H1 and E828-H2, as well as those of the original three samples, were determined using a DuPont 9900 differential scanning calorimeter. The values of T_g determined are shown in Table II.

TABLE II Glass transition temperature, T_g, tensile and bending strengths, and the limiting bending stress, σ_s^c, of specimens

Samples	T_g (°C)	Tensile strength (MPa)	Bending strength (MPa)	σ_s^c(MPa)
E825	135	82.7	227	210
E828	127	82.1	218	180
E834	127	68.8	183	160
E828-H1	138	87.7	–	–
E828-H2	128	82.6	–	–

3.2. Comparison between static and cyclic plane-bending fatigue tests

A relationship between the time-to-failure, t_s, and stress given to specimens, σ, in static bending fatigue tests (S–t curve) is given in Fig. 2. There appears to be a critical stress, σ_s^c, below which the specimen does not show any fatigue failure under a static load, though we did not extend our observation beyond 1800 h. Although the critical values are so close to the bending strengths of the specimens that it is difficult to determine the critical stress exactly, the critical value appears to be in the vicinity of 83–95% of the bending strength of the specimen. The approximate values of σ_s^c of three samples, at least, below which specimens were not fractured for 1800 h, are shown in Table II. The speculation that there would be a critical stress in static fatigue may be confirmed by the following fact: unbroken rod specimens in static fatigue tests are sharply bent if they are taken out of the fatigue test instrument before fracture, and continue to keep their shape almost indefinitely at room temperature. However, it can be observed that bent rods, which have kept the shape for months, can return to the original straight rods if they are placed in an oven at their glass transition temperatures for about 1 h. Thus, it is certain that a deformation in shape occurs due to quasi-plastic flow if a load is given to an epoxy resin rod, but there would be no essential damage in its structure if the stress is below its critical value, σ_s^c. That is, the main chains of network structure are not broken if the specimen is not fractured. The critical stress may correspond to the threshold stress intensity factor, K_{th}, in the crack propagation rate versus stress intensity factor relationship. No crack growth is observed if the stress is below K_{th}. The conclusion that epoxy resins do not show any static fatigue failure below a critical stress, σ_s^c, appears to be in agreement with the experimental results obtained with some kinds of epoxy

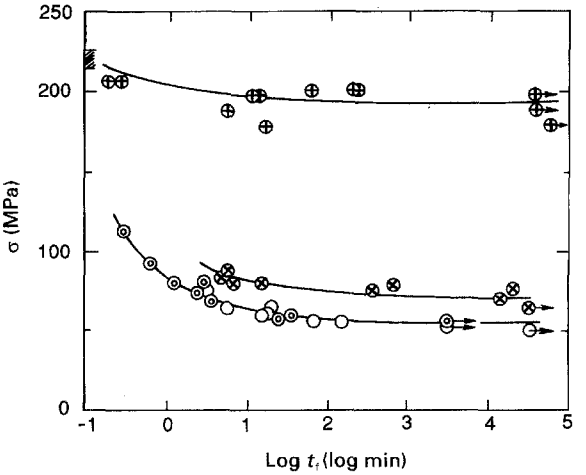

Figure 2 Comparison between the stress, σ, vesus time-to-failure, t_s, relationships (S–t curves) in static and cyclic plane-bending fatigue tests. Sample E828-o. The surfaces of the specimens were as-machined by a lathe. (⊕) Data in static bending fatigue tests, (⊗) data in cyclic plane-bending fatigue tests (1800 cycles /min). (○, ◎) rotary-bending fatigue test data (300 r.p.m.) in air and in argon, respectively, The short arrows show the unfractured specimens throughout the present paper. The bending strength is shown by a hatched zone at log $t_f = -1$.

resins [2], but in disagreement with others. In some experiments, which appear to be in contradiction with the present data [9], however, the investigators observed the lifetimes of cracked specimens, whereas our observations are made on plane surfaces.

In contrast to their behaviour in static fatigue, epoxy resin rods are easily fractured if a cyclic loading is given to the specimens, even though the stresses are far below their critical values in static fatigue, σ_s^c. The data in cyclic plane-bending fatigue tests for the same sample as used in static fatigue tests are plotted in the form of an S–t curve in Fig. 2, for comparison with the data in static bending fatigue. It is clear that the present samples are much more easily fractured in cyclic plane-bending fatigue tests than in static fatigue tests. This means that the fatigue failure is not due to the defects originally existing on the surface of specimen, but due to defects created on the surface by repeated loading. The data in rotary-bending fatigue tests for the same sample are also shown for reference in Fig. 2.

3.3. Rotary-bending fatigue

The data for specimens with different surface roughnesses in rotary-bending fatigue tests are compared in the form of stress, σ, versus cycles-to-failure, N_f, (S–N curve) in Fig. 3. Although the specimens with smooth surfaces are more resistant to cyclic deformation than the specimens with rough surfaces, all specimens show similar fatigue performance, independent of surface roughness in cyclic fatigue tests. It is likely that the failures of both specimens with smooth and rough surfaces were caused by the same mechanism. It is understandable that the lifetime in rotary-bending fatigue tests is affected by surface roughness, even though the mechanism is common. Various reasons may be conceivable; for example, the effective stresses working on rough surfaces are higher than those on smooth surfaces.

The temperature on the surface of the specimen was somewhat raised during the rotary-bending fatigue tests, and the temperature rise was larger with higher rotation speed and also with higher stress. However, it was confirmed that the temperature rise was within several degrees in the present range of stresses at room temperature if the rotation speed was 300 or 600 r.p.m. Such a degree of temperature rise would have little effect on the fatigue performance of the present samples. Some effect was found if the temperature was as high as 100 °C, as shown in Fig. 4.

The S–N curves for the samples with different degrees of cross-linking are compared in Fig. 5. There is no meaningful difference between them, in contrast to the fact that the critical stress in static fatigue, as well as the tensile and bending strengths, is dependent of the degree of cross-linking.

Some specimens of sample E828 were carefully annealed to improve the state of segment packing (sample E828-H1). The lifetimes of the specimens in rotary-bending fatigue tests are compared with those of the specimens cooled in the usual way (sample E828-H2) in Fig. 6. Considering that experimental error is rather high in the low-cycle fatigue region, it may be concluded that sample E828-H1, which was carefully annealed, is more resistant to cyclic deformation than sample E828-H2, which was cooled as rapidly as usual.

Finally, it was also confirmed that the S–N curves in an argon atmosphere were almost identical to those in air, showing that the cyclic bending fatigue of epoxy

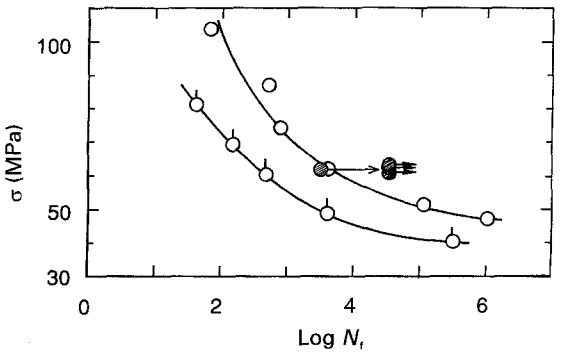

Figure 3 Effects of surface roughness on the stress, σ, versus cycles-to-failure, N_f, relationship (S–N curves) and effects of interruption on the cycles-to-failure, N_f, in rotary-bending fatigue tests (300 r.p.m.). Sample E828, (○) as-machined by a lathe, (○) finished with 1000 and 1500 sandpapers. (◉) The number of cycles at which the rotary-bending fatigue was interrupted; (◉) the number of cycles after ten repeated interrupted tests.

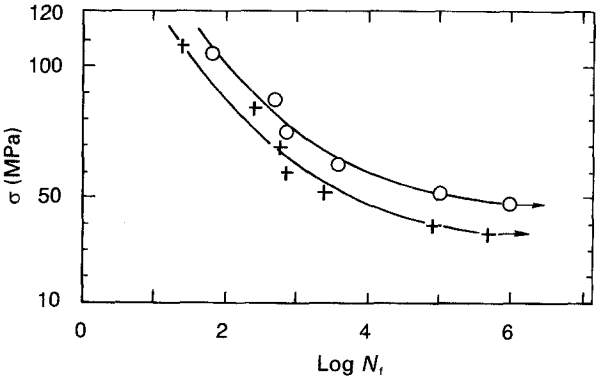

Figure 4 Temperature effects on the S–N curve of E828 specimens in rotary-bending fatigue tests (300 r.p.m.), (○) at room temperature (19–22 °C), (+) at 100 °C.

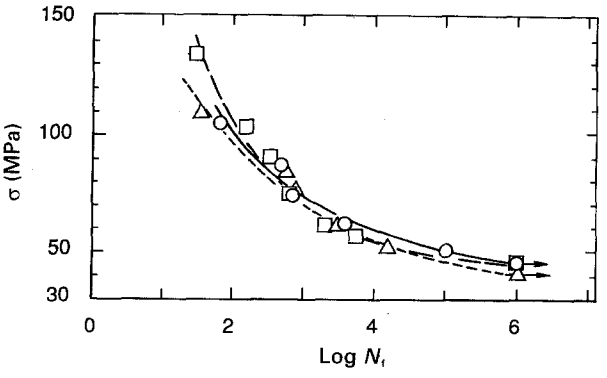

Figure 5 Comparison of the S–N curves of three series of specimens in rotary-bending fatigue tests (300 r.p.m). (△) E825, (○) E828, (□) E834.

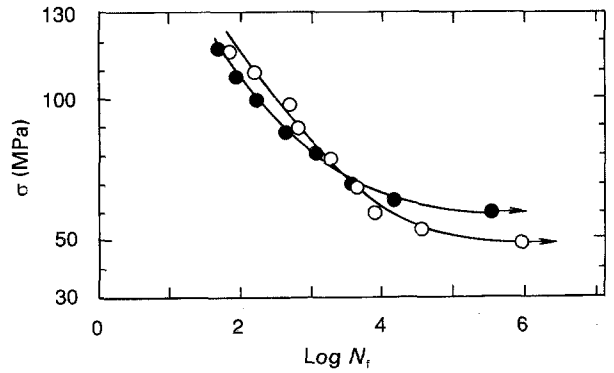

Figure 6 Comparison of the S–N curves of annealed samples (E828-H1 and -H2) in rotary-bending fatigue tests (300 r.p.m.). (●, ○) Data of E828-H1 and -H2, respectively.

resins is neither due to oxidation by air nor due to hydrolysis with vapour in air.

3.4. Observation of fracture surfaces and fatigue crack initiation

The fracture surfaces in cyclic bending fatigue are clearly different from those in static fatigue as well as from those fractured by bending tests. An example of a scanning electron micrograph of a fracture surface created in rotary-bending fatigue tests is shown in Fig. 7. Though not always as clear as in Fig. 7, most fracture surfaces show three regions for the nucleation of a crack, its propagation and the final fracture of the specimen. The crack nuclei can be clearly observed on the surface. The crack nucleation does not start from extended flaws inside the material, but occurs on the surface.

Careful examination of the specimen surface with microscopes reveals that even the surfaces finished with sandpapers are not, naturally, perfectly smooth under the microscopes, but no special defects which could be considered to be responsible for the fracture of the specimen could be found. The same is true for the specimens which were tested for a long time as long as they are not fractured.

To determine when an initial crack nucleus appears, rotary-bending fatigue tests were stopped just before break-down of the specimens (E828-o), and their tensile strengths, σ_B, were determined. Then, we obtained $\sigma_B = 95$ MPa after a test of 1700 cycles at a stress of 79 MPa, at which the specimen is expected to be fractured at about 2100 cycles, and $\sigma_B = 87$ MPa after a test of 200 cycles at a stress of 89 MPa, at which the specimen is expected to be fractured at about 210 cycles. Those values of σ_B are almost equal to the σ_B value of virgin specimens ($\sigma_B = 89$ MPa). Although there is a considerably large ambiguity in the expected cycles-to-fracture, N_f, it seems certain that no damage is caused in the specimens until close to fracture.

Moreover, rotary-bending fatigue tests of three specimens were interrupted when the tests had proceeded by 80% of the expected cycles-to-failure, N_f, of those specimens. Then, two specimens were allowed to rest for one night, one at room temperature and another at the glass transition temperature. The surface

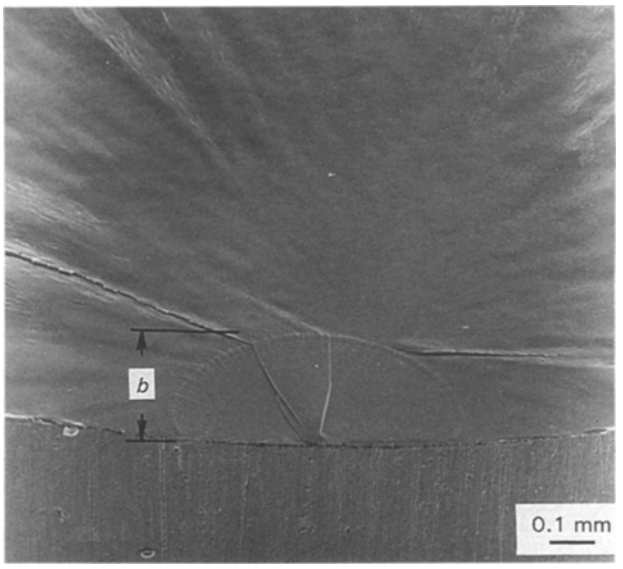

Figure 7 Scanning electron micrograph of a fracture surface in rotary-bending fatigue tests. Sample E828. $\sigma = 62$ MPa. $N_f = 4.1 \times 10^3$.

of the third specimen was polished with no. 1500 sandpaper as at the beginning of the test. After these treatments, those specimens were again given the same rotary-bending fatigue tests. Furthermore, the same treatments were repeated ten times for each specimen. The number of cycles at 80% of the expected cycles-to-failure, N_f, and also the total number of cycles after ten repetitions of the test are shown in Fig. 3, in comparison with the ordinary S–N curve of the specimen. Despite the fact that the total number of cycles of ten repeated tests is eight times higher than the average lifetime of the specimen, N_f, none of the three specimens were fractured. Because it is inconceivable that no fatigue is accumulated for the first 80% N_f, it is reasonable to assume that the fatigue accumulated for the period is reversible so that it may be healed if the specimen is allowed to have a rest. It may be concluded that the nucleation of a fatal crack and its propagation would occur just an instant before the visible failure of the specimen. In addition, it was confirmed under a metallurgical microscope that no visible defects were created on the surfaces of those specimens before the specimen was fractured.

3.5. Propagation of a crack

In cyclic bending fatigue tests, a crack nucleus is thus created on the surface and the crack propagates, causing the final failure of the specimen. The propagation rate is already known to follow Equation 1 [1, 2]. It is also known from fracture mechanics that the depth of the slow crack growth region, b, as denoted in Fig. 7, is correlated with the maximum stress, σ_{max}, such as

$$K_{fC} = \sigma_{max} (\pi b)^{1/2} F \quad (3)$$

where K_{fC} is the critical stress intensity factor in fatigue [10] and F is the shape factor which can be estimated from a table given elsewhere [11]. In the present experiments, the value of F is about 0.70. If a fracture toughness can be defined for the present

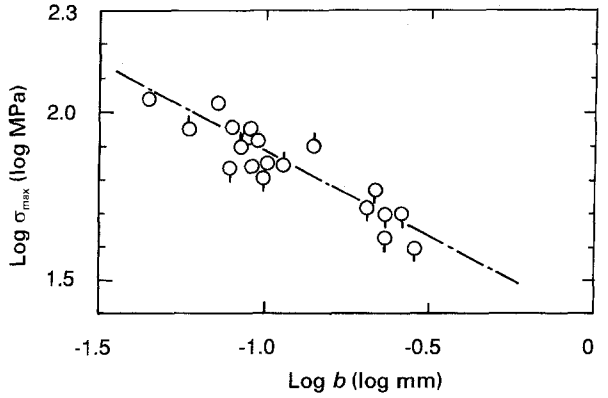

Figure 8 Examples of double logarithmic plots of the maximum stress σ_{max} versus depth of slow crack growth region, b. Sample E828-o. Three different symbols denote the data for three groups of specimens having different surface roughness. The chain line denotes the slope of $-1/2$.

sample, that is, if K_{fC} is a constant, a linear relationship with the slope of $-1/2$ is expected to hold between log σ_{max} and log b.

Fig. 8 shows an example of double logarithmic plots of σ_{max} and b for a sample. It may be concluded that K_{fC} is constant and its average value is about 0.93 MPa $m^{1/2}$. Moreover, it may be pointed out that the critical stress intensity factor K_{fC} is independent of surface roughness, as it should be. The values of b can be unambiguously determined in some cases such as in Fig. 7, but may include some ambiguities in some other cases. However, the ambiguities are not as serious as those affecting the present conclusion. Summarizing the literature and the present experimental results, it may be concluded that, in rotary-bending fatigue tests of epoxy resins, a fatal crack created as a result of repeated deformations propagates following the fracture mechanics of elastic materials and causes the final fracture of the specimen if the maximum stress intensity factor reaches a critical value, K_C. It is expected that K_{fC} may be different with different samples if they have different tensile strengths. However, the expectation could not be confirmed in this work.

4. Discussion

It is thus certain that the rotary-bending fatigue proceeds by way of crack nucleation, propagation of the crack and final failure of the specimen, in agreement with previous work [1]. The time-to-failure, t_s, or cycles-to-failure, N_f, are mainly determined by the time or cycles required for incubation of a crack. This also appears to agree with most previous observations [1, 2]. Once a crack nucleus is created on the surface, the specimen is, practically speaking, instantly fractured, though it may take some time for propagation of the crack. The propagation rate of a crack and the final failure of a specimen proceeds following the general theory of fracture mechanics of elastic materials. Therefore, an important unsolved problem in rotary-bending fatigue of epoxy resins may be in the mechanism of initial crack nucleation, as discussed in Section 1.

Two kinds of force must be broken for fracture of epoxy resin rods to occur. One is the primary covalent bond in the main chain, which forms a network structure in the material, and the other may be the secondary force such as van der Waals' force and dipole interaction working between unbonded segments. Because the three samples, E825, E828 and E834, have different degrees of cross-linking, that is, different numbers of main chains, crossing unit area, it is reasonable that they have different mechanical strengths as well as different critical stresses in static fatigue. E825 is the strongest, E828 the second and E834 is the weakest.

However, it can be observed in Fig. 5 that the three samples with different degrees of cross-linking show little difference in the S–N curve. That is, the degree of cross-linking has little relationship with the lifetime of the specimen in rotary-bending fatigue. As discussed above, the incubation of a crack consumes most of the lifetime of a specimen in rotary-bending fatigue tests, and, moreover, no main chains are broken during the incubation period. Therefore, it is reasonable that the degree of cross-linking has little effect on the lifetime in rotary-bending fatigue.

The factor controlling the lifetime in rotary-bending fatigue tests may be the secondary forces working between unbonded segments or the state of segment packing on the surface. This speculation is supported by the experimental results that E828-H1 and -H2 are made of the same material but, nevertheless, the former is more resistant to cyclic deformation than the latter, clearly because the segments on the surface of the former are more densely packed than the latter. Here, however, it is to be noted that the present experimental data do not mean that the lifetime of epoxy resins in rotary-bending fatigue tests is not affected by the degree of cross-linking, in general. It was reported by Murakami *et al.* [12, 13] that the lifetime of epoxy resins in rotary-bending fatigue tests increases with increasing degree of cross-linking. The present samples were chosen to have different degrees of cross-linking but to have little effect on the cohesive energies among the segments.

Because there is a clear correlation between stress and cycles-to-failure, it is certain that a kind of fatigue or strain is being accumulated until a crack nucleus is created on the surface. However, the present data show that the fatigue or strain accumulated is reversible. This is a remarkable difference from the crack nuclei on metal surfaces, on which an irreversible fatigue is gradually accumulated with number of cycles. Although we could not confirm the reversible strain by observation, it seems certain that a reversible strain may be accumulated in the state of arrangement of unbonded segments, but the distorted segment arrangement can return to the original state due to the contractile force of the network structure, if the cyclic deformation is stopped. If the reversible strain turns into an irreversible defect, it cannot return to the original state but would initiate a crack. Such a transition seems to be possible in epoxy resins,

considering that epoxy resins are in a glassy state and have interstitial vacancies or holes inside. Irreversible transitions might be induced in such vacancies.

Acknowledgements

We thank Mr Toshihisa Shimo and Mr Mitsuru Naruta for their helpful co-operation in experiments, and Dr Akira Ueno for his advice.

References

1. R. J. YOUNG in "Developments in Polymer Fracture-1", edited by E. H. Andrews (Applied Science, 1979), Ch. 6.
2. A. J. KINLOCH and R. J. YOUNG, "Fracture Behavior of Polymers" (Elsevier Applied Science, 1983) p. 316.
3. A. MURAKAMI, H. MATSUSHITA, T. YOSHIKI and M. SHIMPO, *Nihon Sechaku Kyokai Shi* **4** (1983) 135.
4. P. J. E. FORSYTH, *Acta Metall.* **11** (1963) 703.
5. S. A. SUTTON, *Eng. Fract. Mech.* **6** (1974) 587.
6. T. KOIKE and R. TANAKA, *J. Appl. Polym. Sci.* **42** (1991) 1333.
7. A. J. KOVACS, *J. Polym. Sci.* **30** (1958) 131.
8. *Idem, Fortschr. Hochpolym. Forsch.* **3** (1965) 2259.
9. R. A. GLENDHILL and A. J. KINLOCH, *Polymer* **17** (1976) 727.
10. H. TADA, "The Stress Analysis of Cracks Handbook" (Del. Research Corporation, Hellertown, PA, 1973).
11. Y. MURAKAMI and H. TSURU, "Stress Intensity Factors Handbook" (Society of Materials Science, Japan, 1986).
12. A. MURAKAMI, T. YOSHIKI, M. OCHI and M. SHIMPO, *Kobunshi Ronbunshu* **39** (1982) 557.
13. A. MURAKAMI, H. MATSUSHITA, T. YOSHIKI and M. SHIMPO, *Nihon Sechaku Kyokai Shi* **19** (1983) 529.

Received 7 January
and accepted 11 August 1994